PROCEEDINGS OF SCIENCE

Electroweak corrections to Higgs boson pair production: The quark channel

Marco Bonetti,[a,b,c] **Gudrun Heinrich,**[b] **Philipp Rendler**[b,*] **and William J. Torres Bobadilla**[d]

[a] *Institute for Theoretical Physics, University of Tübingen, Auf der Morgenstelle 14, 72076 Tübingen, Germany*

[b] *Institute for Theoretical Physics, Karlsruhe Institute of Technology (KIT), Wolfgang-Gaede-Str. 1, 76131 Karlsruhe, Germany*

[c] *Institute for Astroparticle Physics, Karlsruhe Institute of Technology (KIT), 76344 Eggenstein-Leopoldshafen, Germany*

[d] *Department of Mathematical Sciences, University of Liverpool, Liverpool L69 3BX, U.K.*

E-mail: marco.bonetti@uni-tuebingen.de, gudrun.heinrich@kit.edu, philipp.rendler@kit.edu, torres@liverpool.ac.uk

We present the mixed QCD-electroweak corrections to Higgs boson pair production in the quark–antiquark channel. The virtual amplitudes are computed fully analytically using the method of differential equations. We determine the integration constants by matching our expressions to the large mass expansion limit of the canonical integrals. We implement the results in the POWHEG-BOX framework for phenomenological studies. The corrections are found to have a significant impact on the shapes of differential cross sections, reaching up to +10% for the invariant mass distribution of the Higgs boson pair near the production threshold. This channel has not been considered before in calculations of the next-to-leading order electroweak corrections to Higgs boson pair production.

Loops and Legs in Quantum Field Theory (LL2026)
12-17, April, 2026
Bayreuth, Germany

*Speaker

© Copyright owned by the author(s) under the terms of the Creative Commons Attribution-NonCommercial-NoDerivatives 4.0 International License (CC BY-NC-ND 4.0) All rights for text and data mining, AI training, and similar technologies for commercial purposes, are reserved. ISSN 1824-8039 . Published by SISSA Medialab.

arXiv:2606.25928v1 [hep-ph] 24 Jun 2026

1. Introduction

Constraining the trilinear Higgs coupling is one of the primary goals of the High Luminosity phase of the LHC. Current constraints from the combined ATLAS and CMS analysis at the 95% confidence level, $-0.71 < \lambda/\lambda_{SM} < 6.1$ [1], still allow for significant deviations from the Standard Model prediction, leaving room for beyond-the-Standard-Model physics.

Higgs boson pair production is the primary channel for measuring the trilinear Higgs coupling, as the value of λ directly affects both the total cross section and the shape of differential distributions. Precise theoretical predictions are therefore essential.

QCD corrections to Higgs boson pair production in gluon fusion have been computed at next-to-leading order (NLO) with full top mass dependence [2–6], including parton shower matching [7–12], and up to N^{3}LO + N^{3}LL with the highest order contribution calculated in the heavy-top limit [13–18]. These calculations reduce the residual QCD scale uncertainty to approximately $\mathcal{O}(3\%)$. The top-mass renormalisation scheme uncertainty [10, 19], which remains the dominant uncertainty at the level of $\mathcal{O}(20\%)$, is currently under investigation and has been addressed in Refs. [20, 21].

With the QCD uncertainties substantially reduced, NLO electroweak (EW) corrections become increasingly relevant. These corrections have been shown to contribute at the level of $\mathcal{O}(5\%)$ to the total cross section and up to $\mathcal{O}(30\%)$ for differential distributions [22]. In addition to the full EW corrections, several gauge-invariant subsets have been studied in Refs. [23–32].

These proceedings review Ref. [33], which presented the first study of EW effects in Higgs boson pair production initiated by a quark–antiquark pair. Although these contributions are negligible at the level of the total cross section, they were shown to lead to significant distortions of differential distributions close to the production threshold.

2. Amplitude Calculation

We consider Higgs boson pair production with an incoming quark–antiquark pair,

$$q\overline{q} \to HH\,, \tag{1}$$

with massless quarks of the first two generations, $q \in \{u, d, s, c\}$. Furthermore, we assume a diagonal CKM matrix. Under these assumptions, the Higgs bosons can only be produced through their couplings to EW gauge bosons. Representative Feynman diagrams contributing at leading order (LO) and NLO, separated into real-emission and virtual contributions, are shown in Tab. 1.

Since LO and real-emission amplitudes are generated automatically with `GoSam-3` [34–36], the remainder of this section focuses on the analytic calculation of the two-loop virtual corrections.

We generate all relevant Feynman diagrams using `QGRAF` [37] and translate them into analytic expressions with `FORM 4.2`[1] [39] employing the Feynman rules of Ref. [40]. The amplitudes are computed in both the unitary and Feynman gauge for the EW gauge bosons, finding agreement. These choices are particularly convenient, as they lead to the same set of master integrals.

To treat the γ_5 matrices appearing in quark–gauge-boson couplings, we employ naive dimensional regularisation (NDR) [41]. In the present calculation, all γ_5 matrices occur on open fermion

[1] Note, that `FORM 5.0` has since become available [38].

Table 1: Example Diagrams for LO and NLO $q\overline{q} \to HH$.

Leading Order	Next-to-Leading Order QCD	
	real emissions	virtual corrections
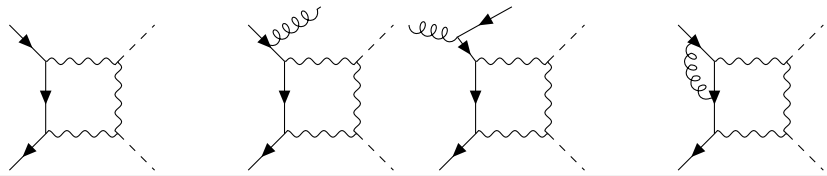		

lines. Consequently, no traces containing γ_5 need to be evaluated in D dimensions, thereby avoiding the ambiguities that may arise in NDR. This allows us to anticommute the γ_5 matrices along the fermion lines and attach them to the external spinors, yielding

$$\overline{v}(p_2)\,\mathcal{M}\,u(p_1) = \overline{v}_L(p_2)\,\mathcal{M}_L\,u_L(p_1) + \overline{v}_R(p_2)\,\mathcal{M}_R\,u_R(p_1)\,. \tag{2}$$

The remaining matrix elements $\mathcal{M}_{L/R}$ are free of γ_5 and can therefore be written in terms of a single form factor,

$$\mathcal{M}_{L/R} \sim \mathcal{F}_{L/R}\not{p}_3\,. \tag{3}$$

For the evaluation of the Feynman integrals, we first use `Reduze 2` [42] and `Kira 3` [43–47] to apply integration-by-parts (IBP) relations and reduce them to a minimal set of 51 master integrals associated with two top-level sectors shown in Fig. 1. The 45 integrals related to the double-box topology, Fig. 1a, were computed by some of us in Ref. [30] using canonical differential equations [48],

$$\mathrm{d}\mathbf{J} = \varepsilon \sum_{i=1}^{51} \mathbb{A}_i \mathrm{dlog}(\alpha_i)\mathbf{J}\,, \tag{4}$$

where $\mathbf{J}$ denotes the canonical integrals, $\alpha_i = \alpha_i(s, t, m_H^2, m_{W/Z}^2)$ are algebraic functions of the kinematic scales, $\mathbb{A}_i$ are rational matrices and ε is the dimensional regulator.

This form was achieved by first constructing a canonical basis using `DlogBasis` [49] for sectors up to six propagators, and a loop-by-loop approach [50] for the top sectors containing seven propagators. The corresponding differential equations were derived with the help of `LiteRed` [51] and `FiniteFlow` [52] and subsequently brought into dlog form with the help of `Efforteless` [53]. The boundary constants were fixed by evaluating the integrals in the large mass expansion, which corresponds to the limit $s, t, u, m_H^2 \ll m_{W/Z}^2$.

The remaining six integrals of the second topology, which is shown in Fig. 1b, involve the same set of integration kernels and were brought into dlog form within the same framework.

Having expressed all master integrals in terms of iterated integrals over logarithmic kernels, we perform additional basis rotations to a set of graded transcendental functions [54, 55]. These functions are constructed by determining linear relations among the integrals order by order in the dimensional regulator ε using `FiniteFlow`. Applying these relations allows us to obtain a minimal set of independent functions at each order in ε .

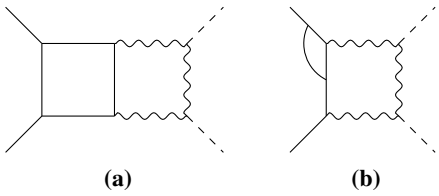

Figure 1: Top sectors of the virtual NLO. Straight lines indicate massless particles, curved lines EW bosons with mass $m_{W/Z}$ and dashed lines Higgs bosons with mass m_H.

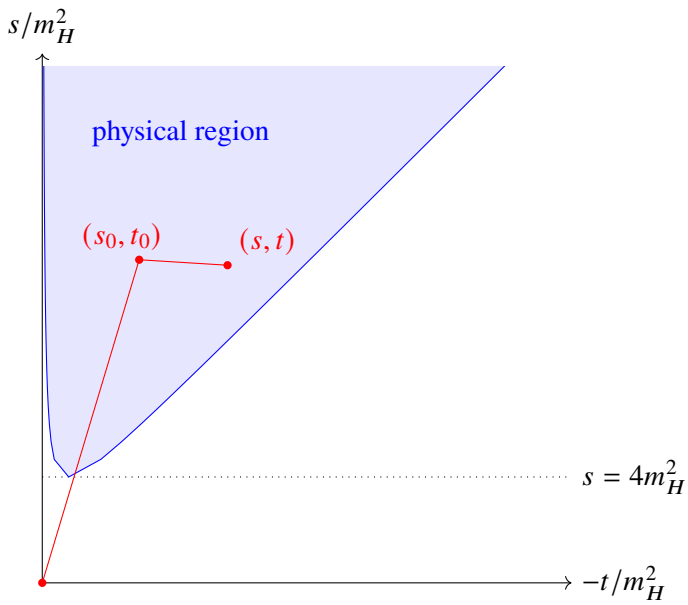

Figure 2: Schematic illustration of the integration path used to evaluate the independent functions.

Expressing the amplitude in terms of independent functions removes all artificial poles. The remaining UV poles are treated by renormalising the strong coupling constant α_s in the $\overline{MS}$ scheme, and the IR poles are removed using the Catani subtraction scheme [56].

To evaluate the independent functions numerically in the physical region, we solve their differential equations using `DiffExp` [57]. As an integration path, we choose two straight segments, as schematically shown in Fig. 2. The first segment connects the large mass limit to a reference point in the physical region,

$$\left\{s_0, t_0, u_0, m_{H,0}^2, m_{W/Z,0}^2\right\} = \left\{\frac{3125}{256}, -\frac{1875}{512}, -\frac{1875}{512}, \frac{625}{256}, 1\right\} . \tag{5}$$

This part of the path is evaluated once and cross-checked against `AMFlow` [58, 59]. The reference point is then used as a starting point for the second segment to explore the physical region.

This split of the integration path ensures that all kinematic thresholds, which lie outside the physical region and may otherwise slow down the numerical integration, are crossed only once during the evaluation of the reference point.

Table 2: EW input parameters used for phenomenological results.

m_H [GeV]	m_W [GeV]	m_Z [GeV]	G_F [GeV^{-2}]
125	80.36	91.1876	0.116639×10^{-4}

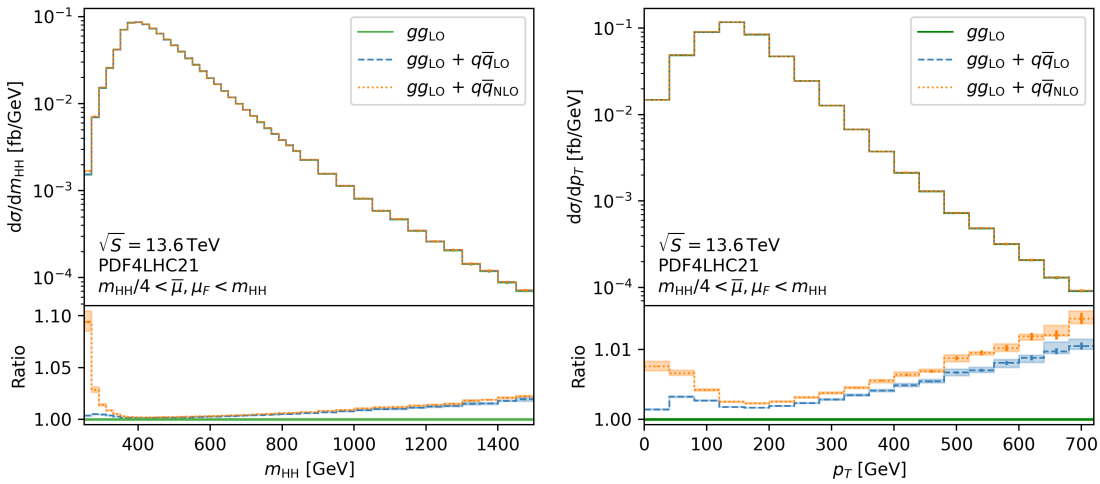

(a) **(b)**

Figure 3: Invariant mass distribution of the Higgs boson pair (a) and transverse momentum distribution of a single Higgs boson (b). The error bands represent the scale uncertainty, while the error bars show the statistical error from the Monte Carlo simulation.

The amplitude can be evaluated in this way with a precision of 16 significant digits in approximately $O(1')$ per phase space point. As this is not sufficiently fast for a direct implementation into `POWHEG-BOX-V2` [60–62], we construct an interpolation grid comprising $O(20\,000)$ phase-space points. Therefore, we compute a rectilinear grid in the parameters

$$\beta = \sqrt{1 - 4\,\frac{m_H^2}{s}} \in [0, 1[\quad \text{and} \quad \cos\theta = \frac{t-u}{s\,\beta} \in [-1, 1]\,, \tag{6}$$

with a sampling density weighted according to the amplitude squared.

The LO amplitudes as well as the real-emission contributions are evaluated on the fly using `GoSam-3`.

3. Results

We calculate differential distributions for a center-of-mass energy of $\sqrt{S} = 13.6\,\mathrm{TeV}$ using the EW input parameters listed in Tab. 2. The renormalisation and factorisation scales are chosen dynamically as $m_{HH}/2$, where m_{HH} denotes the invariant mass of the Higgs boson pair. The scale uncertainties are estimated through 7-point scale variations.

Fig. 3a shows the invariant mass distribution of the Higgs boson pair. The LO and NLO quark–antiquark contributions are shown as dashed blue and dotted orange lines, respectively, together

with the LO gluon-fusion channel, represented by the solid green line. The NLO quark–antiquark channel exhibits a significant enhancement close to the production threshold, reaching a relative correction of approximately +10% compared to LO gluon-fusion. This effect is mainly driven by real-emissions, since the emitted parton softens the spectrum, which leads to a higher population of the threshold region. At larger invariant masses, the NLO corrections remain positive and reach approximately +3%.

Fig. 3b shows the transverse-momentum distribution of one of the Higgs bosons. The corrections exhibit a pattern similar to that observed for the invariant-mass distribution: An enhancement at low transverse momentum, predominantly driven by real-emission contributions, and a moderate increase in the high-p_T tail.

4. Conclusion

These proceedings reviewed the calculation of the quark–antiquark channel for Higgs boson pair production up to NLO QCD. The amplitudes were computed analytically, using differential equations to express Feynman integrals in terms of iterated integrals over logarithmic kernels. Boundary conditions were obtained from a large-mass expansion, and additional basis rotations were performed to construct a basis of graded transcendental functions. The resulting amplitudes were evaluated on a grid using `DiffExp` and implemented into `POWHEG-BOX` for phenomenological studies.

We observe that the quark–antiquark channel has a sizeable impact on differential distributions, even though its contribution to the total cross section is negligible. In particular, the invariant-mass distribution of the Higgs boson pair shows an enhancement of nearly +10% in the threshold region, as well as noticeable Sudakov-type effects at high energies.

Future work includes the public release of the `POWHEG` implementation and a detailed study of the interplay between additional EW and QCD contributions to Higgs boson pair production.

Acknowledgments

This work is supported by the *Deutsche Forschungsgemeinschaft* (DFG, German Research Foundation) under grant no. 396021762 - TRR 257, and by the Leverhulme Trust, LIP-2021-014.

References

[1] CMS, ATLAS collaboration, G. Aad et al., *Combination of ATLAS and CMS searches for Higgs boson pair production at $\sqrt{s}$ = 13 TeV*, 2602.23991.

[2] S. Borowka, N. Greiner, G. Heinrich, S. P. Jones, M. Kerner, J. Schlenk, U. Schubert and T. Zirke, *Higgs Boson Pair Production in Gluon Fusion at Next-to-Leading Order with Full Top-Quark Mass Dependence*, *Phys. Rev. Lett.* **117** (2016) 012001, [1604.06447].

[3] S. Borowka, N. Greiner, G. Heinrich, S. P. Jones, M. Kerner, J. Schlenk and T. Zirke, *Full top quark mass dependence in Higgs boson pair production at NLO*, *JHEP* **10** (2016) 107, [1608.04798].

[4] J. Baglio, F. Campanario, S. Glaus, M. Mühlleitner, M. Spira and J. Streicher, *Gluon fusion into Higgs pairs at NLO QCD and the top mass scheme*, *Eur. Phys. J. C* **79** (2019) 459, [1811.05692].

[5] J. Davies, G. Heinrich, S. P. Jones, M. Kerner, G. Mishima, M. Steinhauser and D. Wellmann, *Double Higgs boson production at NLO: combining the exact numerical result and high-energy expansion*, *JHEP* **11** (2019) 024, [1907.06408].

[6] J. Baglio, F. Campanario, S. Glaus, M. Mühlleitner, J. Ronca, M. Spira and J. Streicher, *Higgs-Pair Production via Gluon Fusion at Hadron Colliders: NLO QCD Corrections*, *JHEP* **04** (2020) 181, [2003.03227].

[7] G. Heinrich, S. P. Jones, M. Kerner, G. Luisoni and E. Vryonidou, *NLO predictions for Higgs boson pair production with full top quark mass dependence matched to parton showers*, *JHEP* **08** (2017) 088, [1703.09252].

[8] S. Jones and S. Kuttimalai, *Parton Shower and NLO-Matching uncertainties in Higgs Boson Pair Production*, *JHEP* **02** (2018) 176, [1711.03319].

[9] G. Heinrich, S. P. Jones, M. Kerner, G. Luisoni and L. Scyboz, *Probing the trilinear Higgs boson coupling in di-Higgs production at NLO QCD including parton shower effects*, *JHEP* **06** (2019) 066, [1903.08137].

[10] E. Bagnaschi, G. Degrassi and R. Gröber, *Higgs boson pair production at NLO in the POWHEG approach and the top quark mass uncertainties*, *Eur. Phys. J. C* **83** (2023) 1054, [2309.10525].

[11] J. Davies, K. Schönwald, M. Steinhauser and D. Stremmer, *ggxy: A flexible library to compute gluon-induced cross sections*, *Comput. Phys. Commun.* **320** (2026) 109933, [2506.04323].

[12] S. Alioli, G. Marinelli and D. Napoletano, *NNLO+PS double Higgs boson production with top-quark mass corrections in GENEVA*, *JHEP* **09** (2025) 206, [2507.08558].

[13] M. Grazzini, G. Heinrich, S. Jones, S. Kallweit, M. Kerner, J. M. Lindert and J. Mazzitelli, *Higgs boson pair production at NNLO with top quark mass effects*, *JHEP* **05** (2018) 059, [1803.02463].

[14] D. de Florian, M. Grazzini, C. Hanga, S. Kallweit, J. M. Lindert, P. Maierhöfer, J. Mazzitelli and D. Rathlev, *Differential Higgs Boson Pair Production at Next-to-Next-to-Leading Order in QCD*, *JHEP* **09** (2016) 151, [1606.09519].

[15] J. Grigo, J. Hoff and M. Steinhauser, *Higgs boson pair production: top quark mass effects at NLO and NNLO*, *Nucl. Phys. B* **900** (2015) 412–430, [1508.00909].

[16] L.-B. Chen, H. T. Li, H.-S. Shao and J. Wang, *Higgs boson pair production via gluon fusion at N^3LO in QCD*, *Phys. Lett. B* **803** (2020) 135292, [1909.06808].

[17] L.-B. Chen, H. T. Li, H.-S. Shao and J. Wang, *The gluon-fusion production of Higgs boson pair: N^3LO QCD corrections and top-quark mass effects*, *JHEP* **03** (2020) 072, [1912.13001].

[18] A. A H and H.-S. Shao, *N^3LO+N^3LL QCD improved Higgs pair cross sections*, *JHEP* **02** (2023) 067, [2209.03914].

[19] J. Baglio, F. Campanario, S. Glaus, M. Mühlleitner, J. Ronca and M. Spira, *$gg \to HH$: Combined uncertainties*, *Phys. Rev. D* **103** (2021) 056002, [2008.11626].

[20] S. Jaskiewicz, S. Jones, R. Szafron and Y. Ulrich, *The structure of quark mass corrections in the $gg \to HH$ amplitude at high-energy*, *JHEP* **09** (2025) 015, [2501.00587].

[21] J. Davies, K. Schönwald and M. Steinhauser, *Three-loop large-N_c virtual corrections to $gg \to HH$ in the forward limit*, *JHEP* **08** (2025) 192, [2503.17449].

[22] H.-Y. Bi, L.-H. Huang, R.-J. Huang, Y.-Q. Ma and H.-M. Yu, *Electroweak Corrections to Double Higgs Production at the LHC*, *Phys. Rev. Lett.* **132** (2024) 231802, [2311.16963].

[23] S. Borowka, C. Duhr, F. Maltoni, D. Pagani, A. Shivaji and X. Zhao, *Probing the scalar potential via double Higgs boson production at hadron colliders*, *JHEP* **04** (2019) 016, [1811.12366].

[24] M. Mühlleitner, J. Schlenk and M. Spira, *Top-Yukawa-induced corrections to Higgs pair production*, *JHEP* **10** (2022) 185, [2207.02524].

[25] J. Davies, G. Mishima, K. Schönwald, M. Steinhauser and H. Zhang, *Higgs boson contribution to the leading two-loop Yukawa corrections to $gg \to HH$*, *JHEP* **08** (2022) 259, [2207.02587].

[26] J. Davies, K. Schönwald, M. Steinhauser and H. Zhang, *Next-to-leading order electroweak corrections to $gg \to HH$ and $gg \to gH$ in the large-m_t limit*, *JHEP* **10** (2023) 033, [2308.01355].

[27] W. Bizoń, U. Haisch, L. Rottoli, Z. Gillis, B. Moser and P. Windischhofer, *Addendum to: Constraints on the quartic Higgs self-coupling from double-Higgs production at future hadron colliders [JHEP 10 (2019) 267]*, *JHEP* **02** (2024) 170, [2402.03463].

[28] G. Heinrich, S. Jones, M. Kerner, T. Stone and A. Vestner, *Electroweak corrections to Higgs boson pair production: the top-Yukawa and self-coupling contributions*, *JHEP* **11** (2024) 040, [2407.04653].

[29] J. Davies, K. Schönwald, M. Steinhauser and H. Zhang, *Analytic next-to-leading order Yukawa and Higgs boson self-coupling corrections to $gg \to HH$ at high energies*, *JHEP* **04** (2025) 193, [2501.17920].

[30] M. Bonetti, P. Rendler and W. J. Torres Bobadilla, *Two-loop light-quark Electroweak corrections to Higgs boson pair production in gluon fusion*, *JHEP* **07** (2025) 024, [2503.16620].

[31] A. Bhattacharya, F. Campanario, S. Carlotti, J. Chang, J. Mazzitelli, M. Mühlleitner, J. Ronca and M. Spira, *Higgs-Pair Production via Gluon Fusion: Top-Yukawa- and light-quark-induced electroweak Corrections*, 2512.14823.

[32] J. Davies, K. Schönwald, M. Steinhauser and H. Zhang, *Analytic next-to-leading order electroweak corrections to Higgs boson pair production at high energies*, 2603.08789.

[33] M. Bonetti, G. Heinrich, P. Rendler and W. J. Torres Bobadilla, *NLO QCD corrections to the electroweak production of a Higgs boson pair in the quark-antiquark channel*, *JHEP* **04** (2026) 131, [2601.16924].

[34] GoSam collaboration, G. Cullen, N. Greiner, G. Heinrich, G. Luisoni, P. Mastrolia, G. Ossola, T. Reiter and F. Tramontano, *Automated One-Loop Calculations with GoSam*, *Eur. Phys. J. C* **72** (2012) 1889, [1111.2034].

[35] GoSam collaboration, G. Cullen et al., *GOSAM-2.0: a tool for automated one-loop calculations within the Standard Model and beyond*, *Eur. Phys. J. C* **74** (2014) 3001, [1404.7096].

[36] J. Braun, B. Campillo Aveleira, G. Heinrich, M. Höfer, S. P. Jones, M. Kerner, J. Lang and V. Magerya, *One-loop calculations in effective field theories with GoSam-3.0*, *SciPost Phys. Codeb.* **62** (2026) 1, [2507.23549].

[37] P. Nogueira, *Automatic Feynman Graph Generation*, *J. Comput. Phys.* **105** (1993) 279–289.

[38] J. Davies, T. Kaneko, C. Marinissen, T. Ueda and J. A. M. Vermaseren, *FORM Version 5.0*, 2601.19982.

[39] B. Ruijl, T. Ueda and J. Vermaseren, *FORM version 4.2*, 1707.06453.

[40] J. C. Romao and J. P. Silva, *A resource for signs and Feynman diagrams of the Standard Model*, *Int. J. Mod. Phys. A* **27** (2012) 1230025, [1209.6213].

[41] M. S. Chanowitz, M. Furman and I. Hinchliffe, *The Axial Current in Dimensional Regularization*, *Nucl. Phys. B* **159** (1979) 225–243.

[42] A. von Manteuffel and C. Studerus, *Reduze 2 - Distributed Feynman Integral Reduction*, 1201.4330.

[43] P. Maierhöfer, J. Usovitsch and P. Uwer, *Kira—A Feynman integral reduction program*, *Comput. Phys. Commun.* **230** (2018) 99–112, [1705.05610].

[44] J. Klappert and F. Lange, *Reconstructing rational functions with FireFly*, *Comput. Phys. Commun.* **247** (2020) 106951, [1904.00009].

[45] J. Klappert, F. Lange, P. Maierhöfer and J. Usovitsch, *Integral reduction with Kira 2.0 and finite field methods*, *Comput. Phys. Commun.* **266** (2021) 108024, [2008.06494].

[46] J. Klappert, S. Y. Klein and F. Lange, *Interpolation of dense and sparse rational functions and other improvements in FireFly*, *Comput. Phys. Commun.* **264** (2021) 107968, [2004.01463].

[47] F. Lange, J. Usovitsch and Z. Wu, *Kira 3: integral reduction with efficient seeding and optimized equation selection*, *Comput. Phys. Commun.* **322** (2026) 109999, [2505.20197].

[48] J. M. Henn, *Multiloop integrals in dimensional regularization made simple*, *Phys. Rev. Lett.* **110** (2013) 251601, [1304.1806].

[49] J. Henn, B. Mistlberger, V. A. Smirnov and P. Wasser, *Constructing d-log integrands and computing master integrals for three-loop four-particle scattering*, *JHEP* **04** (2020) 167, [2002.09492].

[50] W. Flieger and W. J. Torres Bobadilla, *Landau and leading singularities in arbitrary space-time dimensions*, *Eur. Phys. J. Plus* **139** (2024) 1022, [2210.09872].

[51] R. N. Lee, *Presenting LiteRed: a tool for the Loop InTEgrals REDuction*, 1212.2685.

[52] T. Peraro, *FiniteFlow: multivariate functional reconstruction using finite fields and dataflow graphs*, *JHEP* **07** (2019) 031, [1905.08019].

[53] A. Matijašić and J. Miczajka, "Effortless: Efficient generation of odd letters with multiple roots as leading singularities." In preparation.

[54] D. Chicherin, V. Sotnikov and S. Zoia, *Pentagon functions for one-mass planar scattering amplitudes*, *JHEP* **01** (2022) 096, [2110.10111].

[55] T. Gehrmann, J. Henn, P. Jakubčík, J. Lim, C. C. Mella, N. Syrrakos, L. Tancredi and W. J. Torres Bobadilla, *Graded transcendental functions: an application to four-point amplitudes with one off-shell leg*, *JHEP* **12** (2024) 215, [2410.19088].

[56] S. Catani, *The Singular behavior of QCD amplitudes at two loop order*, *Phys. Lett. B* **427** (1998) 161–171, [hep-ph/9802439].

[57] M. Hidding, *DiffExp, a Mathematica package for computing Feynman integrals in terms of one-dimensional series expansions*, *Comput. Phys. Commun.* **269** (2021) 108125, [2006.05510].

[58] X. Liu, Y.-Q. Ma and C.-Y. Wang, *A Systematic and Efficient Method to Compute Multi-loop Master Integrals*, *Phys. Lett. B* **779** (2018) 353–357, [1711.09572].

[59] X. Liu and Y.-Q. Ma, *AMFlow: A Mathematica package for Feynman integrals computation via auxiliary mass flow*, *Comput. Phys. Commun.* **283** (2023) 108565, [2201.11669].

[60] P. Nason, *A New method for combining NLO QCD with shower Monte Carlo algorithms*, *JHEP* **11** (2004) 040, [hep-ph/0409146].

[61] S. Frixione, P. Nason and C. Oleari, *Matching NLO QCD computations with Parton Shower simulations: the POWHEG method*, *JHEP* **11** (2007) 070, [0709.2092].

[62] S. Alioli, P. Nason, C. Oleari and E. Re, *A general framework for implementing NLO calculations in shower Monte Carlo programs: the POWHEG BOX*, *JHEP* **06** (2010) 043, [1002.2581].